Extended Hottel-Whillier Models for uncovered PVT collectors

Mattia Battaglia, Daniel Zenhäusern and Stefan Brunold

SPF Institute for Solar Technology, HSR Rapperswil (Switzerland)

Abstract

Photovoltaic thermal (PVT) collectors are getting more and more attention for their simultaneous production of electricity and low temperature heat. Established mathematical models for the thermal efficiency of thermal collectors as well as the electrical efficiency of PV modules don't include the interactions between the thermal and electrical energy balance. In order to predict efficiencies, we extend the standard Hottel-Whillier collector model to collectors with an additional PV-layer and distinguishable temperature levels for the front side and the back side of the collector. The model is then included in a discrete model of a collector field mounted with a ventilated back side. Based on the field model, we analyze the effect of different sizes of the air gap.

Keywords: Type your keywords here, separated by commas,

1. Introduction

Photovoltaic thermal (PVT) collectors enable the conversion of solar radiation into electrical energy and usable heat (for a review see e.g. [1]). Since they utilize heat, which, in the case of pure PV modules would dissipate, PVT collectors achieve a particularly high level of area-specific energy yield. At the same time, the lower PV cell temperatures lead to higher electrical efficiencies compared to conventional PV modules.

The characterization of PV or thermal components is described in IEC 61215 and EN 12975 / ISO 9806, respectively. In a PVT collector, the thermal and electrical components interact. The maximum amount of solar energy available for heat generation depends on how much of the solar radiation is converted into electrical energy. Photovoltaic efficiency on the other hand depends on the cell temperature, which in turn depends significantly on the fluid temperature. Models for efficiency of pure PV or thermal components do not take these interactions into account and therefore do not describe PVT collectors sufficiently.

A parameterization, which is used for the characterization of products, must find the best possible compromise between simplicity and detail. Several simple models for PVT collectors have been proposed. The model of Florschuetz [2] is based on the assumption that the heat transfer between PV cells and absorber is very good and therefore the cell temperature can be set equal to the absorber temperature. With the model of Stegmann et al. [3] it is assumed that the difference in temperature between PV cells and heat transfer fluid is proportional to the useful heat flow. Another approach, which is used e.g. by the software Polysun [4], is based in equating the cell temperature with the fluid temperature. All these approaches allow a relatively good mapping of the thermal performance of PVT collectors. The quality of the assumptions made to determine the cell temperature depends strongly on the design of the collector. For the quantitative mapping of the additional electrical yield, which results from the cooling of the PV cells, these models are therefore only sufficiently accurate with appropriate restrictions.

We present a simple extension of the Hottel-Whillier model, familiar for pure thermal solar collectors, which can be applied to uncovered PVT collectors. The model allows the identification of new PVT-specific parameters, which allow a good mapping of the PV cell temperature. The parameters can be measured without great additional effort by measuring the cell temperature (via measurement of the open-circuit voltage) during the thermal performance test. For the validation of the model and the determination of the corresponding parameters, indoor and outdoor measurement were carried out.

2. Extensions of the Hottel-Whillier Model

The presented modelling approach is based on the general approach of the Hottel-Whillier-Model [5]. The presented extension has already been published for the special case in which the ambient temperature in the front and the back of the collector can be assumed to be equal [6]. The general geometry of the investigated collector is shown in Figure 1. The collector consists of a front glass, a cell layer, and an absorber structure at the back. The conjunction between the cell layer and the absorber can thereby contain several distinguishable components like protection foils or sheet for stability and heat conduction.

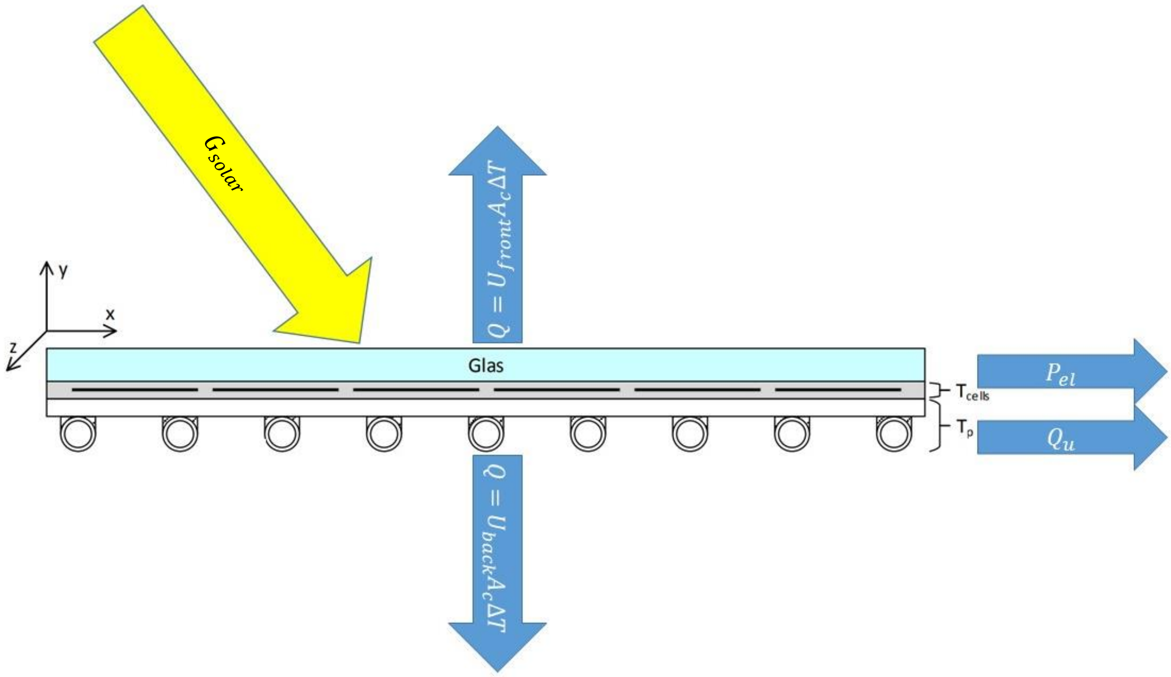

Figure 1 Scheme of the modelled PVT collector.

In the modelling approach of Hottel-Whillier, it is assumed that there is no temperature gradient inside a single layer. Furthermore, the heat conduction in x- and z-direction are treated as independent. In addition, it is assumed that all solar irradiation is absorbed in the cell layer and that the heat conduction in this layer is negligible. Under these assumptions, the energy balance of the cell layer can be represented as

$$G_{eff} = U_{front,conv}\left(T_{cells}(x) - T_{front,amb}\right) + U_{front,rad}\left(T_{cells}(x) - T_{front,lw}\right) + h_{ca}\left(T_{cells}(x) - T_p(x)\right), \quad (1)$$

where the thermal part of the solar gain is defined as the total solar irradiation transmitted through the front glass subtracted by the area specific electrical gain as

$$G_{eff} = \alpha G_{solar} - P_{el}/A_c \quad (2)$$

The local energy balance in the sheet layer of the absorber can be described by

$$\mathrm{k_p}\delta_p \frac{dT_p(x)}{dx} = U_{back,conv}\left(T_p(x) - T_{back,amb}\right) - U_{back,rad}\left(T_p(x) - T_{front,lw}\right) - h_{ca}\left(T_{cells}(x) - T_p(x)\right), \quad (3)$$

where $\mathrm{k_p}$ and δ_p are the heat conductivity and the thickness of the absorber layer respectively. By inserting $T_{cells}(x)$ from Equation (1) into Equation (3) the problem can be rewritten as a second order differential equation in $T_p(x)$

$$\frac{dT_p(x)}{dx} = \frac{U_L}{\mu_{top} k_p \delta_p}\Big(T_p(x) - \frac{U_{back,conv}\mu_{top}}{U_L} T_{back,amb} - \frac{U_{back,rad}\mu_{top}}{U_L} T_{back,lw} - \frac{U_{front,conv}}{U_L} T_{front,amb} - \frac{U_{front,rad}}{U_L} T_{front,lw} - \frac{1}{U_L}\tilde{I}\Big), \tag{4}$$

where U_L is defined as

$$U_L = U_{front,conv} + U_{front,rad} + \mu_{top}\big(U_{back,conv} + U_{back,rad}\big), \tag{5}$$

and μ_{top} is defined as

$$\mu_{top} = \frac{h_{ca} + U_{front,conv} + U_{front,rad}}{h_{ca}}. \tag{6}$$

This differential equation can then be solved by making use of the constraints as shown in [5]. The procedure leads to a final form for the usable energy Q_u in dependency of the fluid temperature T_m

$$Q_u = A_c F' \Big(G_{eff} - U_{front,conv}\big(T_m - T_{front,amb}\big) - U_{front,rad}\big(T_m - T_{front,lw}\big) - \mu_{top} U_{back,conv}\big(T_m - T_{back,amb}\big) - \mu_{top} U_{back,rad}\big(T_m - T_{back,lw}\big)\Big), \tag{7}$$

where the correction factor F' can be considered to be a fin efficiency of the harp-like piping of the absorber. Its mathematical definition is a result of the solution of the differential equation.

$$F = \frac{\tanh\left(\frac{\widetilde{m}(W-D)}{2}\right)}{\frac{\widetilde{m}(\mathrm{W}-D)}{2}} \tag{8}$$

$$F' = \frac{1}{U_L \mathrm{W}\left(\frac{\mu_{top}}{U_L(D + (W-D)F)} + \frac{1}{C_b} + \frac{1}{\pi D h_{fi}}\right)} \tag{9}$$

The additional variables are the distance between two pipes W and the diameter of a single pipe D, the bond conductivity of the junction between absorber sheet and absorber piping C_b, the internal heat transfer coefficient of the fluid flow in the pipe h_{fi}, and $\widetilde{m}$ is defined as

$$\widetilde{m} = \sqrt{\frac{U_L}{\mu_{top} k_p \delta_p}}. \tag{10}$$

3. Parametrization of the thermal efficiency

For uncovered collectors, it is a common practice to include long wave losses in a corrected irradiance value G'' [7]. The corrected value G'' represents the absorbed solar irradiance subtracted by the energy lost by long wave radiation exchange (for the case in which the module is at ambient temperature) depending on the emissivity of the module ϵ and its hemispherical absorption coefficient α for the solar spectrum.

$$G'' = G_{solar} + \frac{\epsilon}{\alpha}(E_L - \sigma T_a^4) \tag{11}$$

Under this approach, the long wave temperature of equation (7) can be replaced by the general ambient temperature. The thermally useful part of G'' can be determined by subtracting the electrical power.

$$G''_{eff} = G'' - \frac{P_{el}}{\alpha A_c} \tag{12}$$

In the following, the thermal efficiency of the PVT collector can be defined as

$$\eta_{\mathrm{th}} = \frac{\mathrm{Q_u}}{A_c G''_{eff}} = \alpha F' - \frac{F'\left(\left(U_{front,conv} + U_{front,rad}\right)\left(T_m - T_{front,amb}\right)\right)}{G''_{eff}} - \frac{F'\mu_{top}\left(U_{back,conv} + U_{back,rad}\right)\left(T_m - T_{back,amb}\right)}{G''_{eff}}. \tag{13}$$

For the special case in which $T_{front,amb} = T_{back,amb} = T_{amb}$, this simplifies to

$$\eta_{\mathrm{th}} = \frac{\mathrm{Q_u}}{A_c G''_{eff}} = \alpha F' - \frac{F' U_L\left(T_f - T_{amb}\right)}{G''_{eff}}, \tag{14}$$

which is of the same form as the parametrization according to ISO 9806

$$\eta_{\mathrm{th}} = \eta_0(1 - b_u u) - (b_1 + b_2 u)\frac{T_m - T_a}{G''_{eff}}. \tag{15}$$

Therefore, in the case of no electrical energy production and $G''_{eff} = G''$, it is possible to link the theoretically determined values of the model directly to the parameters usually measured in collector certifications. If the parameters are only available for measurements with concurrent production of electrical energy, the collector efficiency can be expressed as

$$\eta_{\mathrm{th}} = \frac{\mathrm{Q_u}}{A_c G''} = \frac{\alpha F' G''_{eff}}{G''} - \frac{F' U_L\left(T_f - T_{amb}\right)}{G''} = \alpha F'(1 - \eta_{el}) - \frac{F' U_L\left(T_f - T_{amb}\right)}{G''}. \tag{16}$$

4. Modelling of PVT-Collectors with ventilated back side

The explicit distinction between front and back side ambient temperature and heat transfer values makes it possible to apply the model to a large scale model of a PVT field, whose back side is not insulated but in contact with an air gap. The presence as well as the width of this air gap is dependent on the used mounting system and can also be favorable for the system performance, when the PVT collector should also be used to extract ambient heat as a source for a heat pump. In air gaps of thermal components, natural convection can occur due to temperature differences and change the heat transfer values of the system significantly [8]. Therefore, in such a system the air flow on the back of the PVT-field has to be modelled independently.

A simple approach to model the temperature gradients along the air flow direction is to discretize the PVT collector temperature, the air gap temperature and the roof temperature in z-direction and to use the model of equation (7) for each control volume separately. The discretization of the mounted collector and the air gap is shown in Figure 2. The back side ambient temperatures $T_{back,amb,i}$ can be assumed to be the temperature of the air gap node and the roof temperature can be used as the back side temperatures for the long wave part $T_{back,lw,i}$. For the front side an overall ambient temperature can be used for all control volumes when no temperature differences in z-direction are expected. For the collector fluid with flow rate $\dot{m_f}$ the energy balance between the different control volumes can be formulated as

$$Q_{u,i} = \dot{m}_f c_{p,f}\left(T_{m,i+1} - T_{m,i}\right). \tag{17}$$

The energy balance of the air gap control volume can be represented as

$$\dot{m_{air}} c_{p,air}\left(T_{air,i+1} - T_{air,i}\right) = \frac{U_{back,conv,i} A_c}{N}\left(\overline{T_p} - T_{air,i}\right) + \frac{U_{back,rad,i} A_c}{N}\left(T_{back,lw/wall,i} - T_{air,i}\right), \tag{18}$$

where N is the number of control volumes, A_c the total collector area and $\overline{T_p}$ the average absorber temperature.

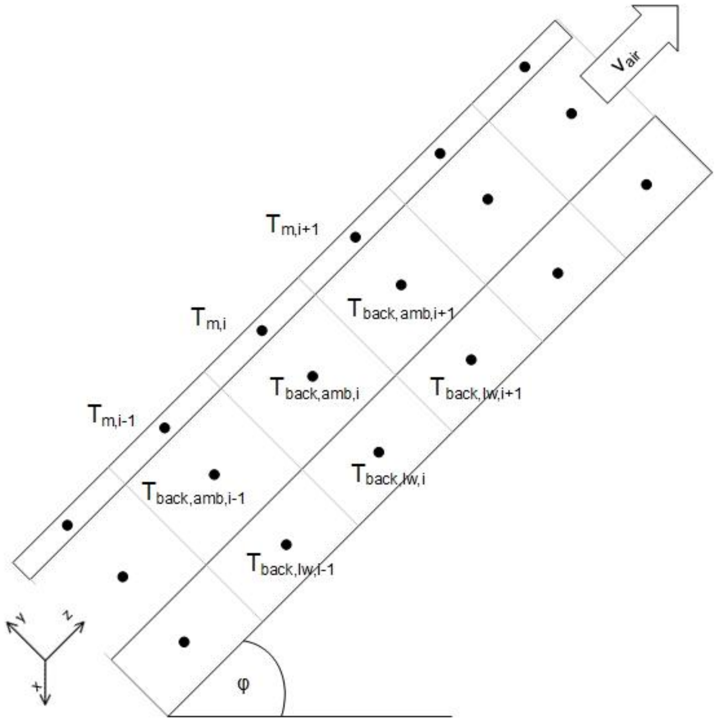

Figure 2 Discretization of the PVT collector field.

For the heat transfer coefficients in the air gap $U_{back,conv,i}$ empirical correlations for internal flows can be used [9].

$$Nu_D = \frac{\left(\frac{f}{8}\right)(Re_D - 1000)Pr}{1 + 12.7\left(\frac{f}{8}\right)^{\frac{1}{2}}(Pr^2 - 1)} \tag{19}$$

The developing natural convection in the air gap can be determined by computing the pressure difference induced by temperature differences between the ambient and the air in the channel. The pressure difference due to buoyancy and friction in one control volume can thus be described by

$$P_i - P_{i+1} = g\Delta z\rho(T)\cos(\phi) \pm \frac{f\rho(T)v^2}{2D_h}, \tag{20}$$

where g is the gravitational acceleration, Δz is the length of a control volume in z direction, f the friction factor, v the air stream velocity and D_h the hydraulic diameter of the air duct. The friction factor can be derived from empirical correlations for the Reynolds number Re_D e.g. [10]:

$$f = (0.790 \ln Re_D - 1.64)^{-2}. \tag{21}$$

The pressure difference between the upper and the lower end of the air gap can then be compared with the difference associated by an equivalent air column with uniform temperature. The resulting pressure difference will be equalized by mass flow according to the dynamic pressure formula

$$\Delta P_{out} = \pm\frac{1}{2}\rho v_{air}^2\,. \tag{22}$$

5. Influence of the ventilated back side

With the resulting model, the effect of different depths of the air gap can be analyzed. An example system with a total height (channel length) of 6 m and an inclination of 60 ° was investigated. The values used in the model equations are shown in Table 1. The absorption coefficient α was chosen such that the model results for $T_m^* = 0$ are equal to Solar Keymark measurement values of a commercially available PVT collector [11].

Table 1 Model parameters

Variable	Description	Value	Unit
$U_{front,conv}$	Front side convective heat transfer rate	2.8	[W/(m²K)]
h_{ca}	Heat transfer coefficient between absorber sheet and PV layer	297	[W/(m²K)]
k	Heat conductivity of the absorber sheet	236	[W/(mK)]
δ_p	Thickness of absorber sheet	$5*10^{-4}$	[m]
W	Separation absorber pipes	0.08	[m]
D	Diameter absorber pipe	0.01	[m]
C_b	Bond conductance absorber sheet/pipe	100	[W/(mK)]
h_{fi}	Internal heat transfer coefficient absorber pipe	300	[W/(m²K)]
σ	Boltzmann constant	$5.67*10^{-8}$	[W/(m²K⁴)]
α	Absorption coefficient PV layer	0.85	[-]
ϵ	Emissivity	0.9	[-]

The results of the model calculation are shown in Figure 3. The collector efficiency values are compared with the values computed from the Solar Keymark Test of the mentioned PVT collector. It can be seen that the computed overall performance of the collector field is similar to the measurement. The model results show that for $T_m^* < 0.02$ all efficiency curves slightly exceed the measured reference. This indicates that at the corresponding temperature levels, the very low level of buoyancy driven flow inside the channel leads to less heat loss on the back side than the free convection present on the experimental test bench. For higher values of T_m^* the calculated efficiency of the PVT collectors mounted on a backside air channel drops below the reference measurement for all depths of the air channel. This can be explained by the increasing air flow due to natural convection that is caused by the larger temperature difference between ambient air and the collector.

On the right hand side of Figure 3 the corresponding average values for the convective heat transfer coefficient between the collector and the air inside the channel is shown. It can be seen that increased temperature differences lead to increased flow and thereby to increased heat transfer rates. In addition, according to the model, the convective heat transfer inside the air channel is increasing for smaller air gap depths.

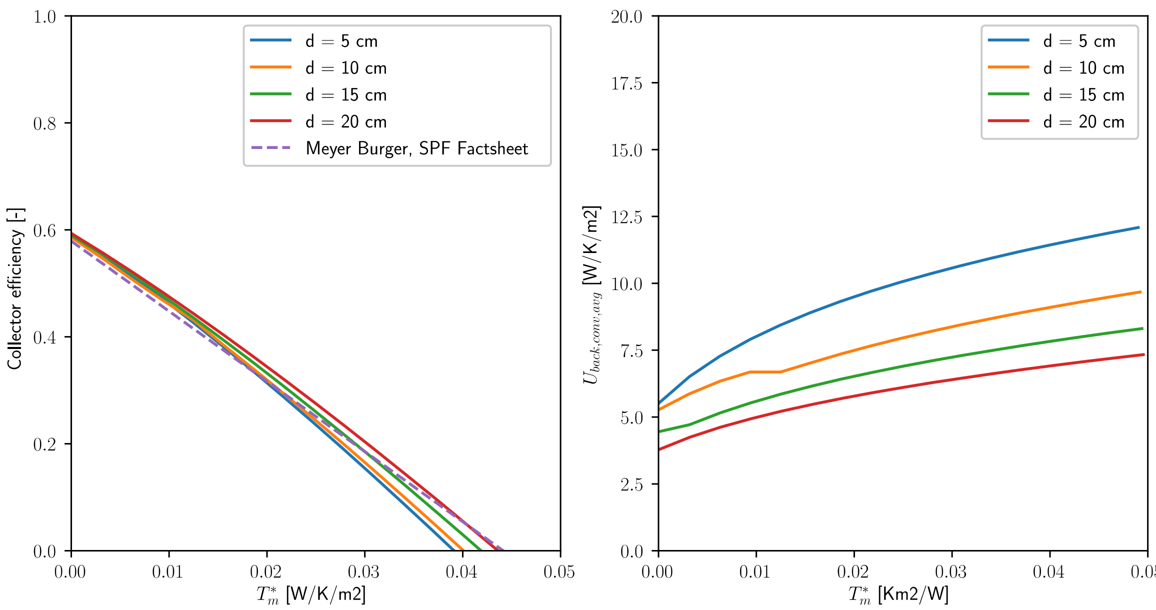

Figure 3 Model results for the inclined PVT field with ventilated back side.

6. Conclusion

We extended the standard Hottel-Whillier-Model to uncovered photovoltaic-thermal collectors. In addition to previous publications we formulated the model equations such that different temperature levels for the front side and the back side of the collector can be used. Based on this extended model for the PVT collector, we modelled a PVT installation with ventilated back side. For the PVT field model we used a simple discretization in the flow direction for both the PVT collector field and the flow in the back side air channel.

The model of the PVT installation with ventilated back side was used to investigate the effect of free convection in an air channel at the back side of a PVT field. The calculations showed that the presence of a ventilated air gap at the back side of the PVT field leads to an increased heat transfer rate especially in the case of high temperature differences between the ambient air and the collector. The effect was found to be increasing for smaller air gaps down to a depth of 5 cm. For systems in which the PVT collectors are used to collect ambient heat, such an installation can be used to enhance the system performance.

7. References

[1] H.A. Zondag, Flat-plate PV-Thermal collectors and systems: A review, Renewable and Sustainable Energy Reviews. 12 (2008) 891–959. doi:10.1016/j.rser.2005.12.012.

[2] L.W. Florschuetz, Extension of the Hottel-Whillier model to the analysis of combined photovoltaic/thermal flat plate collectors, Solar Energy. 22 (1979) 361–366. doi:10.1016/0038-092X(79)90190-7.

[3] M. Stegmann, E. Bertram, G. Rockendorf, S. Janßen, Model of an Unglazed Photovoltaic Thermal Collector Based on Standard Test Procedures, in: Solar World Congress 2011 Proceedings, Kassel, Germany, 2011. https://www.researchgate.net/publication/314383446_Model_of_an_Unglazed_Photovoltaic_Thermal_Collector_Based_on_Standard_Test_Procedures (accessed August 21, 2018).

[4] Software zur Planung von PV-, Solarthermie-, Geothermie- und kombinierte Anlagen - Produktübersicht - Produkt - Vela Solaris AG | Polysun Simulation Software, http://www.velasolaris.com/produkt/produktuebersicht.html (accessed August 21, 2018).

[5] J.A. Duffie, W.A. Beckman, Solar Engineering of Thermal Processes, 4th Edition, Wiley, 2013.

[6] D. Zenhäusern, A. Bohren, M. Rommel, S. Dittmann, T. Friesen, F. Frontini, Thermische und elektrische Charakterisierung von unabgedeckten PVT-Kollektoren, in: 25. OTTI Symposium Thermische Solarenergie, OTTI e.V., Regensburg, Kloster Banz, Bad Staffelstein, Germany, 2015. P:\SPF-Publikationen\2015\150506_OTTI TSE_Bad Staffelstein\Zenhäusern_PVT-Kollektor\Paper\Zenhaeusern_PVT.pdf.

[7] G.L. Morrison, D. Gilliaert, Unglazed Solar Collector Performance Characteristics, Journal of Solar Energy Engineering. 114 (1992) 194–200. doi:10.1115/1.2930005.

[8] D. Faggembauu, M. Costa, M. Soria, A. Oliva, Numerical analysis of the thermal behaviour of ventilated glazed facades in Mediterranean climates. Part I: development and validation of a numerical model, Solar Energy. 75 (2003) 217–228. doi:10.1016/j.solener.2003.07.013.

[9] V. GNIELINSKI, New equations for heat and mass transfer in turbulent pipe and channel flow, Int. Chem. Eng. 16 (1976) 359–368. https://ci.nii.ac.jp/naid/10024972801/ (accessed September 6, 2018).

[10] B.S. Petukhov, Heat Transfer and Friction in Turbulent Pipe Flow with Variable Physical Properties, in: J.P. Hartnett, T.F. Irvine (Eds.), Advances in Heat Transfer, Elsevier, 1970: pp. 503–564. doi:10.1016/S0065-2717(08)70153-9.

[11] Solar Collector Factsheet Meyer Burger Hybrid 280/900 Sky, http://www.spf.ch/fileadmin/daten/reportInterface/kollektoren/factsheets/scf1649de.pdf (accessed September 6, 2018).